

# Step-Wise Deep Learning Models for Solving Routing Problems

Liang Xin , Wen Song , Zhiguang Cao , and Jie Zhang

**Abstract**—Routing problems are very important in intelligent transportation systems. Recently, a number of deep learning-based methods are proposed to automatically learn construction heuristics for solving routing problems. However, these methods do not completely follow Bellman's Principle of Optimality since the visited nodes during construction are still included in the following subtasks, resulting in suboptimal policies. In this article, we propose a novel step-wise scheme which explicitly removes the visited nodes in each node selection step. We apply this scheme to two representative deep models for routing problems, pointer network and transformer attention model (TAM), and significantly improve the performance of the original models. To reduce computational complexity, we further propose the approximate step-wise TAM model by modifying one layer of attention. It enables training on larger instances compared to step-wise TAM, and outperforms state-of-the-art deep models with greedy decoding strategy.

**Index Terms**—Deep learning, deep reinforcement learning, intelligent transportation system, routing problems.

## I. INTRODUCTION

INTELLIGENT transportation system (ITS) has received great attention recently. By combining advanced information technology such as Internet of Things [1], cyber-physical systems [2], and deep learning [3], ITS offers a promising way to improve the safety, efficiency, and sustainability of modern transportation systems [4]. As one of the most fundamental

Manuscript received August 15, 2020; revised October 7, 2020; accepted October 12, 2020. Date of publication October 15, 2020; date of current version April 2, 2021. This work was supported in part by the ST Engineering-NTU Corporate Lab and in part by the Singtel-NTU Cognitive & Artificial Intelligence Joint Lab through the NRF corporate lab/university scheme. The work of Wen Song was supported in part by the Young Scholar Future Plan of Shandong University under Grant 62420089964188. The work of Zhiguang Cao was supported in part by the National Natural Science Foundation of China under Grant 61803104 and in part by the Singapore National Research Foundation under Grant NRF-RSS2016004. Paper no. TII-20-3924. (Corresponding author: Wen Song.)

Liang Xin and Jie Zhang are with the School of Computer Science and Engineering, Nanyang Technological University, Singapore 639798 (e-mail: XINL0003@e.ntu.edu.sg; ZhangJ@ntu.edu.sg).

Wen Song is with the Institute of Marine Science and Technology, Shandong University, Jinan 266237, China (e-mail: wensong@email.sdu.edu.cn).

Zhiguang Cao is with the Department of Industrial Systems Engineering and Management, National University of Singapore, Singapore 119077 (e-mail: zhiguangcao@outlook.com).

Color versions of one or more of the figures in this article are available online at <https://ieeexplore.ieee.org>.

Digital Object Identifier 10.1109/TII.2020.3031409

problems in ITS, *routing problems* aim at planning the paths for one or multiple vehicles so that certain objective (e.g. total travel distance) is optimized. Traveling salesman problem (TSP) and capacitated vehicle routing problem (CVRP) are two typical routing problems, and are of great importance to many real-world applications of ITS [5]. However, routing problems are generally NP-hard combinatorial optimization problems [6]. While exact methods such as branch and bound [7] offer nice theoretical guarantees on the optimality, they suffer from the scalability issue due to their exponential (worst-case) complexity. In contrast, heuristic algorithms often yield suboptimal solutions with much shorter computational time, and hence are more preferred for solving large-scale routing problems in reality. However, traditional heuristic approaches rely on hand-crafted decision rules to guide the solving process, which require substantial domain knowledge and engineering effort to design, and may lead to poor solutions [8].

Recently, researchers have been focusing on using deep learning methods to automatically learn the heuristics for solving routing problems in an end-to-end fashion, without the need of using domain knowledge to design hand-crafted rules [8]–[12]. Most of these methods follow the encoder–decoder paradigm, where the encoder maps the information of locations in the routing problems (e.g., coordinates, demands) into feature embeddings, and the decoder is responsible for incrementally creating the solutions. Among these methods, pointer network (PtrNet) [9] and transformer attention model (TAM) [12] are two representative methods. PtrNet uses long short-term memory (LSTM) [13] as encoder and decoder, and is the first modern deep learning model for combinatorial optimization problems. Motivated by the recent success of transformer [14] in natural language processing, TAM adopts the self-attention-based encoder and decoder, and outperforms a wide range of (traditional or learning-based) algorithms on a series of routing problems.

Essentially, the above methods focus on learning construction heuristics, which extend an empty solution by repeatedly adding locations (or nodes) into the current partial routes until completion. This process can be viewed as a sequence of node-adding decisions [11], since there is no backtracking procedure to modify previous decisions. Therefore, it should follow the Bellman's Principle of Optimality [15] that the optimal policy should only consist of optimal subpolicies. Taking TSP as an example, the salesman sequentially visits cities without repetitions by starting from one city and returning to the same city. The whole problem can be divided into a sequence of subproblems in each of which one city is to be visited. Moreover, given the starting city and the

location of the salesman, the visited cities are no longer relevant to the future subproblems. Inspired by the Bellman's Principle of Optimality, we do not need and should not incorporate any information about the visited cities when solving a (future) sub-problem of TSP. Similarly, these properties also apply to CVRP.

Though existing deep models such as PtrNet and TAM perform well in solving routing problems, they do not completely follow the Bellman's Principle of Optimality. This is because in each decoding step, i.e., for each subproblem, the same node embeddings are used and the irrelevant nodes are not removed. In other words, they are not solving the correct subproblems, and, therefore, may result in suboptimal policies. To address this issue, in this article, we propose *step-wise* deep learning models to solve routing problems. The core idea is that, at each decoding step, we explicitly eliminate the visited and irrelevant nodes in the graph, and extract feature embeddings from the same encoder with different graphs obtained after the elimination operations. We apply this scheme to PtrNet and TAM to demonstrate its effectiveness. Specifically, we propose the step-wise PtrNet (SW-PtrNet) with supervised learning for TSP, and the step-wise TAM (SW-TAM) with reinforcement learning for both TSP and CVRP. However, the step-wise operation is computationally expensive, especially for SW-TAM, since it performs complete reembeddings at each decoding step. To make it more efficient, we propose approximate SW-TAM (ASW-TAM) with reasonable computational overhead, where the top attention layer in the encoder serves as part of the decoder and learns features directly for solving the correct subproblems with irrelevant nodes removed.

We perform extensive experiments to evaluate our methods. Results show that both SW-PtrNet and SW-TAM significantly outperform their respective original models on small problems. Moreover, ASW-TAM enables training on larger instances, and outperforms state-of-the-art deep models with greedy decoding strategy. Note that our aim here is not to compete with highly optimized and specialized solvers (e.g., Concorde for TSP) on a specific problem. Instead, we propose an effective scheme that can improve existing deep models toward automatically learning stronger heuristics, which could exploit the rich data generated in ITS applications and be of great practical value especially when facing new problems with little domain knowledge.

The rest of the article is organized as follows. Section II briefly reviews existing works. Section III introduces the routing problems and the baseline models. Section IV presents our step-wise models in great detail. Section V provides the computational experiments and analysis. Finally, Section VI concludes this article.

## II. RELATED WORK

Motivated by the recent advances of deep learning, researchers have been exploiting the idea of applying deep neural networks to solve challenging combinatorial optimization problems [16], using both supervised and reinforcement learning. Typical deep learning models usually have a fixed output dictionary. However, combinatorial optimization problems such as

TSP and CVRP often have varying sizes, and, therefore, seeking a deep model for solving these problems is tricky. The first deep architecture that satisfies this requirement is PtrNet [9], which resolves the issue of varying output dictionary size by introducing a pointer structure for deep learning models. It considers a combinatorial problem instance as a sequence of input nodes, and uses an LSTM network to encode the sequence and another LSTM to decode the solution.

While PtrNet is trained by supervised learning in [9], Bello *et al.* [10] train PtrNet in the reinforcement learning setting using the policy gradient algorithm. They show that reinforcement learning is effective for training TSP solvers on larger problem sizes with better results. Nazari *et al.* [11] notice that the model should be invariant to the sequence of the input nodes, and replace the LSTM in the encoder of PtrNet with point-wise projection. They train this model also with policy gradient, and present promising results on CVRP.

Different from PtrNet and its variants in [9]–[11] that use LSTM-based sequence-to-sequence models, Kool *et al.* [12] adopt the self-attention mechanism in the recently proposed transformer model [14] for encoding nodes. They train this elegant model (TAM) also with reinforcement learning, using policy gradient with a greedy rollout baseline. On a variety of routing problems including TSP and CVRP, TAM outperforms the methods in [9]–[11] and a wide range of traditional nonlearning-based methods, and is the state-of-the-art deep learning model for routing problems.

With a different scheme, Khalil *et al.* [8] use Structure2Vec [17], a graph-embedding framework to embed the nodes based on the connectivity of the underlying graph. By training with deep Q-network, this model works quite well on some graph combinatorial problems. However, as empirically shown in [12], it does not perform satisfactorily for problems such as TSP and CVRP that are defined on fully connected graphs.

Except [8], all models discussed above fall into the encoder-decoder paradigm, where the encoder processes the nodes in the graph once to get the node embeddings, and the decoder selects one node at each step sequentially to get the solution. However, as we have mentioned, they do not consider the issue of removing the visited nodes that are irrelevant to the remaining subproblems, and therefore, may result in suboptimal policies and relatively large optimality gaps. In contrast, we explicitly eliminate the irrelevant nodes using the step-wise scheme. Even though the computational complexity raises, with elegant approximation, this scheme can yield better performance over the original models with reasonable computational overhead.

Note that it is not clear whether supervised or reinforcement learning is better for combinatorial optimization problems. On the one hand, supervised learning is more well-studied and usually converges faster. On the other hand, reinforcement learning has the advantage of not requiring true labels (i.e., optimal solutions), which could be extremely expensive to obtain for large-scale combinatorial problems. Nevertheless, as will be shown later, our step-wise scheme works well in both supervised and reinforcement learning settings.





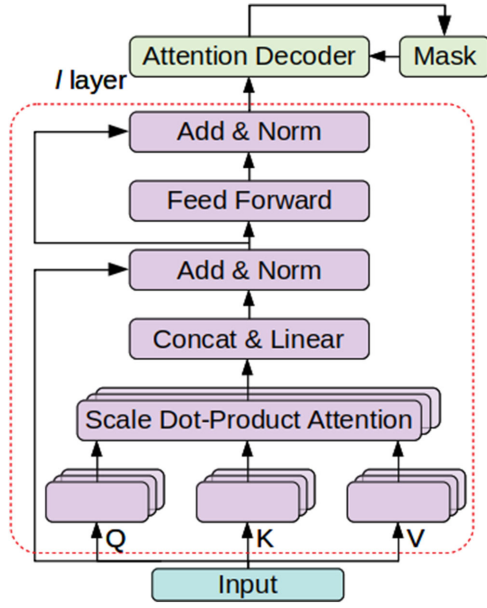


Fig. 2. TAM.

$$\text{Multihead}(Q, K, V) = \text{Concat}(A^1, A^2, \dots, A^H)W_O \quad (6)$$

where  $X^p$  is the input to this layer,  $i$  is the node index,  $h$  is the head index, and  $H$  is the number of heads.  $W_Q^h, W_K^h, W_V^h \in \mathbb{R}^{d \times d_k}$ , and  $W_O \in \mathbb{R}^{d \times d}$  are trainable parameters, and  $d$  is the feature dimension,  $d_k = d/H$ . Here,  $Q, K, V$  are linear projections of node embeddings and represent the Query, Key, Value vector according to the rationale of self-attention [14]. The self-attention block works as follows:

$$\hat{f}_i = \text{BN}(X_i + \text{Multihead}_i(Q, K, V)) \quad (7)$$

$$f_i = \text{SelfAttention}_i(X^p) = \text{BN}(\hat{f}_i + \text{FF}(\hat{f}_i)) \quad (8)$$

where  $f$  is output of the self-attention block, and FF is two feed-forward layers with ReLu activation. Both (7) and (8) have a skip-connection [27] and a Batch Normalization layer [28].

The decoder models  $P(y_t|X, y_1, \dots, y_{t-1})$  use an attention mechanism as follows:

$$f_c = \text{Concat}(\text{Mean}(f), f_{y_0}, f_{y_{t-1}}) \quad (9)$$

$$f_c^g = \text{Multihead}(W_Q^g f_c, W_K^g f^t, W_V^g f^t) \quad (10)$$

$$q = W_Q f_c^g, k_i = W_K f_i \quad (11)$$

$$o_i = C \tanh(q^T k_i / \sqrt{d}), i \in U_t \quad (12)$$

$$P(y_t|X, y_1, \dots, y_{t-1}) = \text{softmax}(o) \quad (13)$$

where  $f^t$  is node embeddings and  $d$  is feature dimension. Here,  $o$  is similar to  $u^t$  in (3). In (9), for the first step,  $f_{y_0}$  and  $f_{y_{t-1}}$  are replaced by trainable parameters. And (10) is similar to the glimpse in [29] with a multhead attention to get a new context.  $C = 10$  is used to clip  $o_i$  to  $[-10, 10]$  for better exploration [10]. The structure of TAM is shown in Fig. 2, where the purple and green boxes are the operations running only once and at every decoding step, respectively.

## IV. MODELS

In this section, we describe our approach in detail. We first show how to apply the step-wise scheme to PtrNet and TAM. Then, we present the approximate SW-TAM which can reduce the computational overhead of the step-wise TAM.

### A. Step-Wise PtrNet

Clearly in PtrNet,  $p_\theta(y_t|y_1, \dots, y_{t-1}, X; \theta)$  is a function of all nodes in the input  $X$ . In other words, while selecting one node to visit, the node embeddings depend on the whole graph including the already visited nodes. However, the previous decisions in the solution construction process cannot be altered and should not affect the future decisions. Therefore, with the irrelevant information of the visited nodes for the embeddings, the model may not produce an optimal policy for the subproblems at each step. Inspired by the Bellman's Principle of Optimality, we correct this by explicitly eliminating the visited and irrelevant nodes in the graph at each step. More specifically, after one node is selected and visited at step  $t$ , the encoder LSTM reembeds the remaining nodes with this visited node eliminated from the sequence to get new embeddings  $e_i^t$ , instead of simply using the original embeddings  $e_i$ . Note that we do not remove the default starting node  $x_1$ , since the salesman needs to return to  $x_1$  eventually. We call this model step-wise PtrNet (SW-PtrNet).

Here we demonstrate the inference process of SW-PtrNet, i.e., how to reembed the node information and select the next node. In each decoding step  $t$ , the encoder LSTM first embeds each unvisited node  $x_i$  sequentially. The resulting embedding for  $x_i$  is the  $i$ th hidden state in the encoder  $e_i^t = h_i^e = \text{LSTM}_e(x_i, h_{i-1}^e)$ . After that, the decoder computes its hidden state as  $h_t^d = \text{LSTM}_d(y_{t-1}, h_{t-1}^d)$ , where  $y_{t-1}$  is the node selected in step  $t-1$  and  $h_{t-1}^d$  is the memory state from the encoder in step  $t$  (note that the encoder and decoder do not share parameters). Then, the conditional distribution over the next node  $y_t$  can be obtained as follows:

$$u_i^t = v^T \tanh(W_1 e_i^t + W_2 h_t^d), \quad i \in U_t \quad (14)$$

$$p_\theta(y_t|y_{t-1}, y_1, V_t; \theta) = \text{softmax}(u^t). \quad (15)$$

While solving TSP, the model keeps track of the visited nodes and masks them out for the probability of selecting  $y_t$ , i.e., only the nodes  $i \in U_t$  (the set of unvisited nodes) can be selected at step  $t$ . Therefore, the constraint for not visiting the same nodes twice is satisfied. After selecting  $y_t$  based on the above distribution, SW-PtrNet moves to the next step. The visited node  $y_t$  is removed from the input sequence and the encoder LSTM is used to reembed the sequence to get  $e_i^{t+1}$  for the decoder at step  $t+1$ . Therefore, different from  $h_i^e$  in (2), the node embeddings  $e_i^t$  in (14) is reembedded at each step. As a result, the conditional probability in (15) no longer conditions on the previous visited nodes, unlike (3). Since the decoder only decodes one node during each step  $t$ , there is no need to maintain its memory state. The process is repeated until only one node is unvisited. Then, a tour is obtained by appending the unvisited node and the starting node to the sequence, such that the constraints of TSP

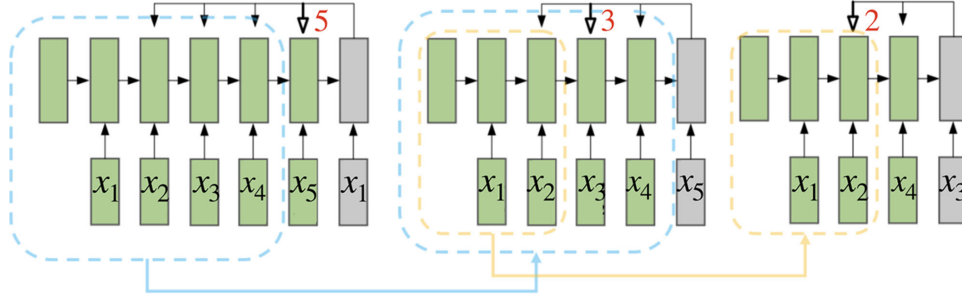


Fig. 3. SW-PtrNet.

**Algorithm 1:** Inferring a Solution Using SW-PtrNet.**Data:** Set of nodes  $X$ **Result:** The solution sequence  $Y$ 

- 1 Embedding sequence with all the nodes using the encoder LSTM;
- 2 **while** not all nodes are visited **do**
- 3 Select the node to visit using the decoder LSTM with (14) and (15);
- 4 Eliminate the selected node and reembed the unvisited nodes using the encoder LSTM.

are satisfied. The process of SW-PtrNet solving a TSP instance with five nodes is shown in Fig. 3.

The algorithm for solving one TSP instance using SW-PtrNet is shown in Algorithm 1. With LSTM reembedding the nodes at each step, the computational complexity of the encoder at inference time raises one order up from  $O(nd^2)$  to  $O(n^2 d^2)$ , where  $d$  is the feature dimension and  $n$  is the number of nodes. This is due to Line 4 in Algorithm 1 which has worst case computation complexity of  $O(nd^2)$  for each of the  $n$  runs. Intuitively, for each step  $t$ , the encoder needs to eliminate  $y_{t-1}$  and reembed all the remaining unvisited nodes. However, we can save some computation by reusing some of the previous embeddings. In fact, the encoder LSTM just needs to truncate right before  $x_s = y_{t-1}$  in the input sequence of step  $t - 1$ , and embed the nodes after  $x_s$ . To achieve this, we keep the first  $s - 1$  embedding steps in the encoder and skip the selected node  $x_s$ . After that, we embed node  $x_{s+1}$  as  $e_{s+1}^t = h_{s+1}^e = \text{LSTM}_e(x_{s+1}, h_{s-1}^e)$ , and other unvisited ones similarly. We illustrate this process in Fig. 3, where the dashed boxes are the embeddings that can be reused. Since a significant amount of computation could be saved, we do not seek an approximation for SW-PtrNet.

**B. Step-Wise TAM**

The original TAM model also suffers from the same issue as PtrNet, i.e., the encoder embeds all nodes only once, and the same embeddings are used throughout decoding, without removing previously visited nodes that are irrelevant to future decisions. Therefore, the embeddings calculated at the beginning are no longer accurate after a couple of steps, resulting in suboptimal policies. Although the glimpse mechanism in (10) tries to correct the context for the query vector  $q$ , the node embeddings to

form this query vector and the key vectors  $k_i$  still correlate with the irrelevant information from the visited nodes. To fix this, we apply the step-wise scheme to TAM, and explicitly make the embeddings independent of the irrelevant nodes. To this end, at each step, the transformer encoder reembeds the whole graph with the irrelevant nodes eliminated. More specifically, we project the nodes linearly with  $X_i^p = W_p x_i$  and run the whole  $L$  layers of self-attention block as (8) in the encoder at each step  $t$  with the irrelevant nodes masked

$$f_i^t = \text{SelfAttention}_i^t(X^p). \quad (16)$$

In the multihead attention of (16), to mask the irrelevant nodes, we compute the attention compatibility  $A^h$  using the following equation instead of (5):

$$w_{ij}^h(Q_i^h, K_j^h) = \begin{cases} Q_i^h K_j^{hT} / \sqrt{d_k}, & j \in U_t \\ -\infty, & \text{otherwise} \end{cases} \quad (17)$$

$$A^h = \text{softmax}(w^h) V^h. \quad (18)$$

Here,  $w_{ij}^h$  is the  $j$ th element of the  $i$ th vector of the matrix  $w^h$  with dimension  $n \times n$  and the softmax in (18) is along the second dimension. As shown in Algorithm 2, after selecting one node to visit at step  $t$  (line 3), the encoder reembeds the new set of feasible nodes  $i \in U_t$  with (16)–(18), and the decoder takes the new embeddings for step  $t + 1$  (line 4). Note that for TSP, the set of feasible nodes  $U_t$  consists of the unvisited nodes; while for CVRP,  $U_t$  consists of unvisited nodes which also satisfy the capacity constraints. The model keeps track of the history of selected nodes to get the set of feasible nodes  $U_t$  for each step  $t$ . And the decoder decodes the probability of selecting next nodes based on the new node embeddings where the probability is masked out for the infeasible nodes  $i \notin U_t$ . Therefore, after all nodes are visited, a feasible solution that satisfies all the constraints for the routing problems (TSP or CVRP) can be obtained.

We call the above model SW-TAM, which is no longer a model for the whole problem but for each subproblem of selecting one node to visit. Its structure is illustrated in Fig. 4 following the same style of Fig. 2. Both TAM and SW-TAM are trained in the reinforcement learning setting, where the model parameters are optimized to maximize the cumulative reward that corresponds to minimizing the total tour length. Following [12], we use standard REINFORCE algorithms with a greedy roll-out baseline. Specifically, the baseline policy is the periodically saved best-performing model parameters. After

**Algorithm 2:** Inferring a Solution Using SW-TAM.

- 1 Embedding the set of nodes using the transformer encoder with (4)–(8);
- 2 **while** not all nodes are visited **do**
- 3 Select the node to visit using the Attention Decoder with (9)–(13);
- 4 Eliminate the infeasible nodes and reembed the nodes with (16)–(18).

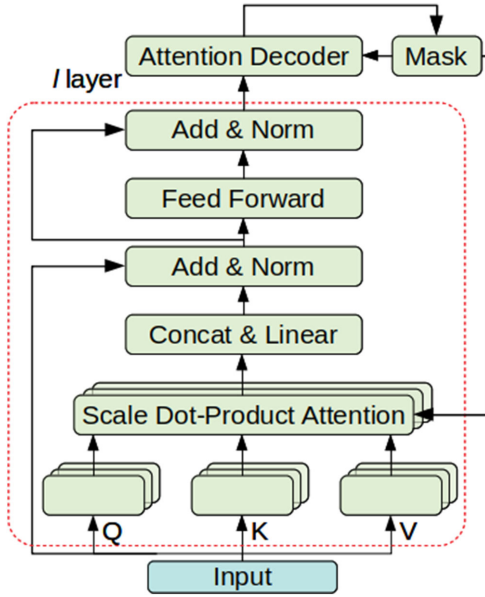


Fig. 4. SW-TAM.

evaluating a held-out dataset at the end of each epoch, the best set of parameters is kept to greedily infer the result as the baseline.

In Algorithm 2, similar to SW-PtrNet, the reembedding operation (Line 4) also introduces additional overhead to SW-TAM. This is due to the fact that the problem with  $n$  nodes breaks into subproblems in each step, where the encoder needs to encode the nodes  $n$  times. The computation complexity of the multihead self-attention block (16) is  $O(nd^2 + dn^2)$  if we consider the number of heads as constant [14]. Due to (16) running for  $n$  times, the computational complexity of the encoder in SW-TAM is  $O(n^2 d^2 + dn^3)$ , which is cubic of the number of nodes and hard to scale up to larger graphs. In the next subsection, we design an approximation of SW-TAM that is more computationally efficient.

### C. Approximate SW-TAM

It is well-known that in convolutional neural network for face recognition, the lower convolutional layer extracts more general features such as lines in different degrees. On the contrary, the upper layer extracts specific features that are more direct for performing the task such as detecting different types of eyes or noses [30]. Based on this intuition, we hypothesize a similar feature extraction paradigm for the attention model, which we

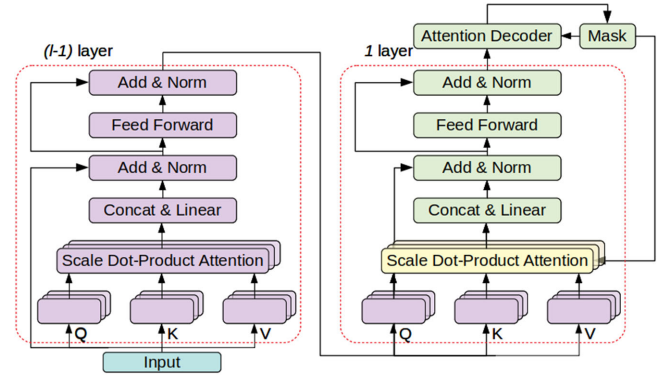


Fig. 5. ASW-TAM.

will validate in the experiments. Below we employ it to achieve better computational efficiency.

More specifically, we propose a new model which approximately performs the reembedding process in SW-TAM by fixing the lower attention layer at each step, and change only the top layer by masking out the attention weights of irrelevant nodes in the multihead attention mechanism. In this new model with  $L$  multihead attention blocks, the first  $L - 1$  is the same as standard building blocks, which can be viewed as the encoder. On the other hand, the top attention layer is part of the decoder, where at each step, the attention mechanism in this layer masks out the irrelevant nodes and gets new embeddings. This design is illustrated in Fig. 5, where the purple boxes are the encoder running only once for embeddings, and the green boxes are the decoder running at each step. The yellow box (multihead attention layer in the last attention block) is also part of the decoder with the attention weights precomputed for once and masked at every step. The first part (precomputation) of the yellow box is defined mathematically as (4) and the following equation:

$$w^h(Q^h, K^h) = Q^h K^{hT} / \sqrt{d_k}. \quad (19)$$

The second part of the yellow box runs at each step  $t$ , and is to set  $w^h_{C_{t-1}} = -\infty$  and perform the following computation and (6)

$$A^h = \text{softmax}(w^h) V^h. \quad (20)$$

Then, the node embeddings are computed using (7) and (8). Based on the new embeddings, the rest part of the decoder selects a new node and gets a new mask. The model will then move to step  $t + 1$  and runs the second part in the yellow box with the new mask. We call this model ASW-TAM. The inferring process for ASW-TAM is shown in Algorithm 3. The constraints can be satisfied using the same procedure as that for SW-TAM.

In this new proposed layer in ASW-TAM, (4) and (19) only need to run once and have the computational complexity of  $O(nd^2)$  and  $O(dn^2)$ , respectively. Equations (4) and (19) and the first  $L - 1$  attention layers run in Line 1 in Algorithm 3. Equations (6)–(8) need to run every decoding step as Line 4 in Algorithm 3 resulting in  $O(n^2 d^2)$  computational complexity in total. Note that straightforward implementation of (20), which

**Algorithm 3:** Inferring a Solution Using ASW-TAM.

- 
- 1 Embedding the set of nodes using the transformer encoder with (4)–(8);
  - 2 **while** not all nodes are visited **do**
  - 3 Select the node to visit using the attention decoder with (9)–(13);
  - 4 Eliminate the infeasible nodes and reembed the nodes approximately with (20) and (6).
- 

will be performed  $n$  times, results in the complexity of  $O(n^3 d)$ . However, with elegant engineering, we managed to achieve  $O(n^2 d)$  for calculation of (20) as shown in the following.

We omit the head index  $h$  for simplicity, and (20) can be explicitly rewritten into element-wise form as follows:

$$\hat{w}_{i,j} = \exp(w_{i,j}), \text{ for all } i \text{ and } j \quad (21)$$

$$A_{i,j} = \frac{\sum_k \hat{w}_{i,k} V_{k,j}}{\sum_k \hat{w}_{i,k}}, \text{ for all } i \text{ and } j. \quad (22)$$

And we define

$$sw_i(t=1) = \sum_k \hat{w}_{i,k}, \text{ for all } i \quad (23)$$

$$swV_{i,j}(t=1) = \sum_k \hat{w}_{i,k} V_{k,j}, \text{ for all } i \text{ and } j. \quad (24)$$

Equations (21), (23), and (24) are precomputed once and have the computation complexity of  $O(n^2 d)$ . At step  $t=1$ , none of the nodes is masked and each element of  $A$  is calculated as follows:

$$A_{i,j} = \frac{swV_{i,j}(1)}{sw_i(1)}, \text{ for all } i \text{ and } j. \quad (25)$$

Then, at step  $t-1$  after decoding, the node with index  $l$  is visited and should be removed. Accordingly, each element of  $A$  at step  $t$  is calculated as follows:

$$sw_i(t) = sw_i(t-1) - \hat{w}_{i,l}, \text{ for all } i \quad (26)$$

$$swV_{i,j}(t) = swV_{i,j}(t-1) - \hat{w}_{i,l} V_{l,j}, \text{ for all } i \text{ and } j \quad (27)$$

$$A_{i,j} = \frac{swV_{i,j}(t)}{sw_i(t)}, \text{ for all } i \text{ and } j. \quad (28)$$

For each element, the computational complexity with respect to each of (25)–(28) is  $O(1)$  and the total number of elements is  $O(nd)$ . Therefore, the computational complexity for each step is  $O(nd)$ , and for all the steps is  $O(n^2 d)$ . Consequently, the total computational complexity of the top attention layer is considered as  $O(n^2 d^2)$ . Note that the equations are written in the element-wise form only for illustration purpose.

Compared to TAM, ASW-TAM raises the computation complexity from  $O(nd^2 + dn^2)$  to  $O(n^2 d^2)$ . However, it is still quadratic in the number of nodes. Even  $d$  could be large as 128, and we only need to do this in the top layer, which turns out to be acceptable as demonstrated in the experiments.

## V. EXPERIMENTS

In this section, we conduct experiments to verify the effectiveness of our step-wise deep learning models on two types of routing problems, i.e., TSP and CVRP.

Following [11], [12], here the locations of TSP and CVRP instances are generated independently from a two-dimensional uniform distribution ranging from 0 to 1 for both dimensions. We generate instances with 20, 50, and 100 nodes for TSP and CVRP. For convenience, we refer them as TSP20, CVRP20, etc. For CVRP, the demands of each node are sampled uniformly from discrete numbers  $\{1 \dots 9\}$  while the vehicle capacities are fixed as 30, 40, and 50 for CVRP20, CVRP50, and CVRP100, respectively. For testing, we generate 10,000 samples from the same distribution and keep it fixed for all models. For training and evaluation, we use the highly optimized solver Concorde [31] to get the optimal solutions for TSP. For CVRP, since it is much harder to be solved optimally, we use the state-of-the-art solver LKH3 [32] to get the benchmark solutions.

### A. SW-PtrNet

In this subsection, we compare SW-PtrNet with the original PtrNet. For a fair comparison, we adopt a similar training scheme and problem settings as in [9], i.e., using supervised training on TSP problems. We use the TSP20 instances for training and testing, as it is the largest training size in [9]. Moreover, with larger problem sizes, the availability of the optimal solutions as training samples is at great expense due to the exponential computational complexity of the exact algorithms. Therefore, we generate 1 600 000 TSP20 instances, and solve them using Concorde to get the optimal solutions for training. On the other hand, the exact algorithm for CVRP is far less efficient than that for TSP, and it is prohibitively time-consuming to generate sufficient optimal solutions as training samples. Therefore, we do not consider CVRP for PtrNet or SW-PtrNet in this subsection.

The models are trained with the Adam optimizer [33] where the learning rate is initially 0.001 and decayed by 0.96 every 5000 steps. We train both models for 1 000 000 iterations with batch size of 128 and clip the gradient by 2.0 of  $L_2$  norm. The coordinates of nodes are projected into a 256 dimension space before being fed into the decoder. The hidden dimension for both the encoder and decoder is 256. The parameters are initialized with uniform distributions in the range of  $[-0.08, 0.08]$ . For TSP, since the route is a loop, the selection of the first node does not matter and is assumed to be known. Thus, for each sampled instance, only 18 selections need to be predicted. During the training for both models, we mask out the output for infeasible selections as shown in (14).

Here we use four measures for evaluation, including the average solution distance, optimality gap, and total inference time on the 10 000 testing instances, as well as training accuracy. We use accuracy here because both models are trained by supervised learning to imitate the construction of optimal (training) solutions. In such setting, accuracy can directly reflect the ability of a model in terms of imitation. We only report training accuracy



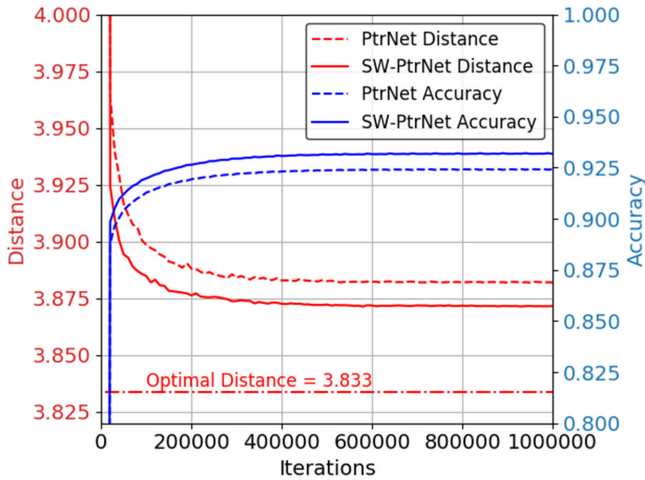


Fig. 6. PtrNet vs SW-PtrNet during training.

TABLE I  
PTRNET VS. SW-PTRNET

Models	Distance	Opt. Gap	Accuracy	Total Time
PtrNet	3.882	1.28%	92.39%	3s
SW-PtrNet	<b>3.872</b>	<b>1.00%</b>	<b>93.17%</b>	14s

The bold entities are the better ones in the comparison (better objective values, smaller optimal gaps, faster inference time).

because it is more informative. Since there exist at least two optimal routes for each TSP instance, testing accuracy could be very low for one of the optimal routes as it can easily be different from the true label. This mismatch is much less severe for training accuracy due to the fixed inputs to the decoder.

In Fig. 6, we plot the performance of PtrNet and SW-PtrNet during training, measured by the testing distance and training accuracy after every 1000 training steps. We can observe from Fig. 6 that SW-PtrNet almost consistently outperforms PtrNet during training in terms of both measures. Training accuracy indeed indicates good performance here, since SW-PtrNet, which is more accurate, consistently produces lower solution distance. We further list the convergence performance in Table I, along with the average optimality gap and the total inference time for the 10 000 testing instances. SW-PtrNet clearly outperforms PtrNet in terms of solution quality. Regarding the optimal gap, the relative improvement for SW-PtrNet over PtrNet is 21.88%. The inference time of SW-PtrNet is longer than PtrNet, which is not surprising since it has higher computational complexity as we have analyzed in Section IV. Nevertheless, both models are very fast since they solve 10 000 instances within 15 s.

To summarize, our step-wise scheme can effectively improve the performance of the original PtrNet in solving TSP.

## B. SW-TAM

In this subsection, we show the effectiveness of SW-TAM by comparing with the original TAM. As mentioned, SW-TAM is computationally expensive; therefore, we use small routing problems here, i.e., TSP20 and CVRP20. For a fair comparison,

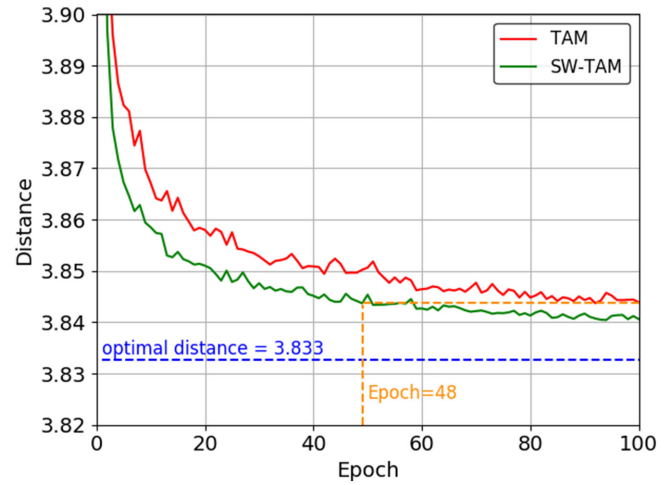


Fig. 7. TAM vs. SW-TAM for TSP 20.

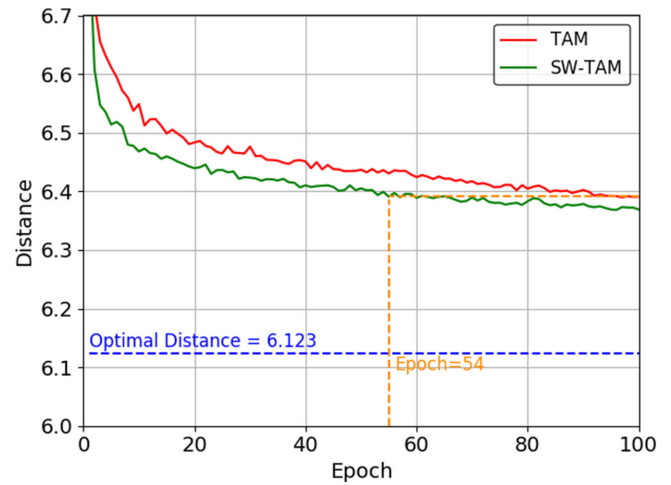


Fig. 8. TAM vs. SW-TAM for CVRP 20.

we use the same setting and hyperparameters as those in the original TAM, and train it using REINFORCE with the greedy rollout baseline for 100 epochs [12]. Each epoch has 1 280 000 instances generated on the fly.

We plot the training curves of greedy decoding TAM and SW-TAM on TSP20 and CVRP20 in Figs. 7 and 8, respectively. As can be observed, SW-TAM is significantly better than the original TAM on both problems. In terms of optimality gap for TSP and CVRP, SW-TAM reduces those of original TAM from 0.29% to 0.19% and 4.46% to 4.15%, respectively. Moreover, it takes only 48 and 54 epochs for SW-TAM to reach the results of TAM after 100 epochs.

However, the computational complexity of reembedding after each step in SW-TAM is one order higher than that of the original model. Regarding TSP and CVRP, it takes 52 and 66 min to train an epoch for SW-TAM, while TAM only needs 6 and 9 min, respectively. Hence, it is hard to scale up to large problems with 50 or 100 nodes due to the memory and time constraints. This motivates us to design the approximate SW-TAM model, which will be evaluated in the next subsection.



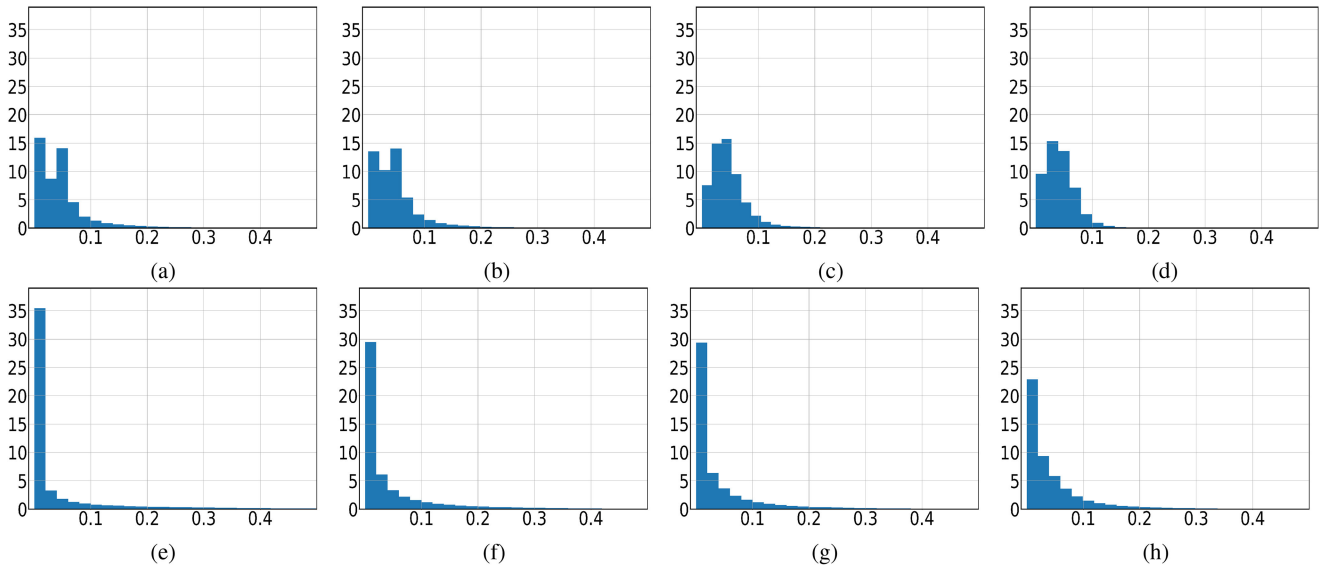


**Fig. 9.** Histograms of attention weights in TAM and ASW-TAM for TSP20 and CVRP20; the coordinates of  $x$ -axis and  $y$ -axis for each bin are the values of attention weights and the percentage frequencies divided by the bin width, respectively. (a) TSP, TAM, bottom. (b) TSP, ASW-TAM, bottom. (c) CVRP, TAM, bottom. (d) CVRP, ASW-TAM, bottom. (e) TSP, TAM, top. (f) TSP, ASW-TAM, top. (g) CVRP, TAM, top. (h) CVRP, ASW-TAM, top.

**TABLE II**

ASW-TAM RESULTS VS. TAM RESULTS. VALUES IN THE PARENTHESES ARE THE TOTAL INFERENCE TIME FOR SOLVING THE 10 000 TESTING INSTANCES

Problem	Opt. Obj.	TAM Obj.	Gap	ASW-TAM Obj.	Gap	Impr. on Gap
TSP20	3.83	3.84 (0s)	0.29%	<b>3.84</b> (1s)	<b>0.23%</b>	20.69%
TSP50	5.69	5.79 (2s)	1.79%	<b>5.76</b> (7s)	<b>1.16%</b>	35.19%
TSP100	7.76	8.10 (6s)	4.35%	<b>8.01</b> (29s)	<b>3.20%</b>	26.39%
CVRP20	6.12	6.40 (1s)	4.46%	<b>6.39</b> (2s)	<b>4.29%</b>	3.66%
CVRP50	10.38	10.98 (3s)	5.82%	<b>10.90</b> (9s)	<b>4.98%</b>	14.40%
CVRP100	15.64	16.75 (8s)	7.07%	<b>16.42</b> (39s)	<b>4.99%</b>	29.44%

The bold entities are the better ones in the comparison (better objective values, smaller optimal gaps, faster inference time).

### C. Approximate SW-TAM

In this subsection, we compare the performance of ASW-TAM with the original TAM on TSP and CVRP instances with 20, 50, and 100 nodes. The training settings are the same as those in the previous subsections.

The results are summarized in Table II. Note that similar to Figs. 7 and 8, these results are based on greedily decoding the model, which is sufficient to prove the effectiveness of our proposed step-wise scheme. However, the solution quality of our model can also be further improved if additional techniques such as sampling or beam search are applied. As can be observed, ASW-TAM consistently outperforms the original TAM model in terms of distance and optimality gap on all instances. The relative improvement is significant for most of these problems. Moreover, the improvement on the optimality gap tends to be larger on harder instances with more nodes. Though the inference time of ASW-TAM is longer than TAM due to the computational overhead of reembedding the nodes approximately, it is still very fast and acceptable as it takes less than 1 min to solve 10 000 instances with 100 nodes. Compared to traditional

nonlearning solvers based on complicated search algorithms, the inference time is still very short and even negligible. For example, Lin–Kernighan–Helsgaun (LKH) [34] takes 13 h to solve 10 000 instances of CVRP100 with 32 parallel threads as shown in [12].

In terms of training efficiency, on TSP20, it takes only 12 min for ASW-TAM to train an epoch, which is significantly less than the 52 min of SW-TAM, and is acceptable compared to the 6 min for the original TAM. This drastic improvement enables us to train ASW-TAM on larger instances with 50 and 100 nodes. For TSP20, the optimality gap of ASW-TAM is 0.23%, which is a bit larger than that of SW-TAM (0.19%). This shows that ASW-TAM trades off performance for better computational efficiency, which validates the effectiveness of our design.

To better understand the rationale of how ASW-TAM works, we plot the weights of the bottom and top attention layers of both TAM and ASW-TAM in solving TSP20 and CVRP20 using histograms in Fig. 9, respectively. We can observe that the pattern of attention weights distribution is clearly different across different layers. More specifically, weight distribution in the bottom layer (layer 1) is flatter in the sense that the attention weights are mostly around 0.05, which is the average weight for 20 nodes, and almost all of the attention weights are within 0.3. In contrast, the distribution of the weights in the top layer (layer 3) is more uneven where 30 percent of the weights are less than 0.02 and the attentions with larger weights are much more than the corresponding proportion of the bottom layer. This observation validates our intuition in Section IV-C. In particular, the lower attention layer extracts more fundamental features of the input instance. On the other hand, the upper layer extracts features that are more directly helpful for solving the problem based on the uneven weight distribution, and is much more aggressive in the sense that it will pay more attention to the informative nodes and barely any attention to irrelevant nodes. Therefore, we keep

**TABLE III**  
ASW-TAM RESULTS VS. TAM RESULTS ON TSPLIB. NUMBER IN THE  
INSTANCE NAME IS ITS SIZE

Instance name	Opt. Obj.	TAM		ASW-TAM		Impr. on Gap
		Obj.	Gap	Obj.	Gap	
berlin52	7542	8898	17.98%	<b>8229</b>	<b>9.11%</b>	49.31%
st70	675	700	3.69%	<b>694</b>	<b>2.80%</b>	24.17%
kroA100	21282	26035	22.33%	<b>24424</b>	<b>14.76%</b>	33.89%
rd100	7910	8490	7.33%	<b>8090</b>	<b>2.27%</b>	69.04%
pr107	44303	51735	16.77%	<b>45625</b>	<b>2.98%</b>	82.21%
kroA150	26524	30356	14.45%	<b>28964</b>	<b>9.20%</b>	36.32%
kroA200	29368	35623	21.30%	<b>34194</b>	<b>16.43%</b>	22.85%
tsp225	3916	4738	21.00%	<b>4709</b>	<b>20.25%</b>	3.57%
pr264	49135	61060	24.27%	<b>54736</b>	<b>11.40%</b>	53.03%
pr299	48191	65320	35.54%	<b>63902</b>	<b>32.60%</b>	8.28%

The bold entities are the better ones in the comparison (better objective values, smaller optimal gaps, faster inference time).

the embeddings from lower layers unchanged in ASW-TAM, and only perform reembedding in the top layer at each decoding step to obtain features that are more related to solving the problems by masking out the visited nodes.

Following [8], we further compare the performance of our model ASW-TAM and the original TAM on 38 instances from a widely used benchmark TSPLIB [35], ranging from 51 to 318 cities. We directly perform inference on these instances using the models trained for TSP100. To get a better generalization performance on these instances with different sizes, the statistics for the batch normalization layer in both models come from instances with the same number of nodes as the one being inferred, which can be computed in advance and introduces no additional computational overhead. Results show that ASW-TAM outperforms TAM with an optimal gap of 12.20% against 14.75%, and finds better solutions for over 76% (29 out of 38) instances. Table III shows the results of 10 selected instances due to limited space. We can observe that ASW-TAM performs well across various problem sizes. The total inference time of the 38 instances for TAM and SW-TAM are 0.56 and 0.89 s, respectively.

TAM, SW-TAM and ASW-TAM are all based on the architecture of transformer. However, it is known that training transformer model could be expensive and may take a significantly long time, even with supervised learning [14]. This has more impacts on the reinforcement learning setting, since the training might converge slowly. Consequently, the 100 training epochs we adopted from [12] previously to train these three models may not yield the best performance. Hence, we train these models for a longer time and notice that they can converge to better results. However, ASW-TAM still shows consistently better performance than the original TAM. Specially, we demonstrate this using TSP20 and TSP50. In TSP20, after 600 training epochs, TAM converges to an average distance of 3.838 with optimality gap of 0.14%, and ASW-TAM converges to 3.837 with optimality gap of 0.10%. For TSP50, TAM takes 1000 epochs to converge to an average distance of 5.739 with optimality gap of 0.82%, while ASW-TAM converges after 800 epochs to an average distance of 5.722 with optimality gap of 0.52%. The relative improvements on the optimality gap are 27% and 37%,

respectively, which are roughly the same as the result for 100 epochs in Table II. All our experiment codes are available<sup>1</sup>.

## VI. CONCLUSION

In this article, we proposed a step-wise scheme for the deep models that learn construction heuristics to solve routing problems. In this scheme, the nodes that were visited in the construction process were explicitly eliminated, such that the following subproblems were correctly represented. We then applied this scheme to PtrNet and TAM, two representative deep models, and obtained significant improvements in terms of optimality. To ameliorate the expensive computation caused by the reembedding operations in SW-TAM, we further proposed the ASW-TAM by modifying the last attention layer, which significantly reduced the complexity and retained good empirical performance. For future work, we would like to apply this step-wise scheme to other models and on other problems. Also, we hope that this idea would inspire further researches on designing network architectures considering the recursive nature of sequential decision-making problems.

## REFERENCES

- [1] K.-H. N. Bui and J. J. Jung, "Aco-based dynamic decision making for connected vehicles in IoT system," *IEEE Trans. Ind. Informat.*, vol. 15, no. 10, pp. 5648–5655, Oct. 2019.
- [2] Y. Feng, B. Hu, H. Hao, Y. Gao, Z. Li, and J. Tan, "Design of distributed cyber-physical systems for connected and automated vehicles with implementing methodologies," *IEEE Trans. Ind. Informat.*, vol. 14, no. 9, pp. 4200–4211, Sep. 2018.
- [3] M. Veres and M. Moussa, "Deep learning for intelligent transportation systems: A survey of emerging trends," *IEEE Trans. Intell. Transp. Syst.*, vol. 21, no. 8, pp. 3152–3168, Aug. 2020.
- [4] D. Li, L. Deng, Z. Cai, B. Franks, and X. Yao, "Intelligent transportation system in Macao based on deep self-coding learning," *IEEE Trans. Ind. Informat.*, vol. 14, no. 7, pp. 3253–3260, Jul. 2018.
- [5] X. Wang, T.-M. Choi, H. Liu, and X. Yue, "Novel ant colony optimization methods for simplifying solution construction in vehicle routing problems," *IEEE Trans. Intell. Transp. Syst.*, vol. 17, no. 11, pp. 3132–3141, Nov. 2016.
- [6] D. L. Applegate, R. E. Bixby, V. Chvatal, and W. J. Cook, *The Traveling Salesman Problem: A Computational Study*. Princeton, NJ, USA: Princeton Univ. Press, 2006.
- [7] M. Fischetti, P. Toth, and D. Vigo, "A branch-and-bound algorithm for the capacitated vehicle routing problem on directed graphs," *Oper. Res.*, vol. 42, no. 5, pp. 846–859, 1994.
- [8] E. Khalil, H. Dai, Y. Zhang, B. Dilkina, and L. Song, "Learning combinatorial optimization algorithms over graphs," in *Proc. Adv. Neural Inf. Processing Syst.*, Red Hook, NY, USA, 2017, pp. 6348–6358.
- [9] O. Vinyals, M. Fortunato, and N. Jaitly, "Pointer networks," in *Proc. Adv. Neural Inf. Process. Syst.*, Cambridge, MA, USA, 2015, pp. 2692–2700.
- [10] I. Bello, H. Pham, Q. V. Le, M. Norouzi, and S. Bengio, "Neural combinatorial optimization with reinforcement learning," in *Proc. 5th Int. Conf. Learn. Representations*, Toulon, France, 2016.
- [11] M. Nazari, A. Oroojlooy, L. Snyder, and M. Takác, "Reinforcement learning for solving the vehicle routing problem," in *Proc. Adv. Neural Inf. Process. Syst.*, Red Hook, NY, USA, 2018, pp. 9839–9849.
- [12] W. Kool, H. van Hoof, and M. Welling, "Attention, learn to solve routing problems!" in *Proc. 7th Int. Conf. Learn. Representations*, New Orleans, LA, USA, 2018.
- [13] S. Hochreiter and J. Schmidhuber, "Long short-term memory," *Neural Comput.*, vol. 9, no. 8, pp. 1735–1780, 1997.
- [14] A. Vaswani et al., "Attention is all you need," in *Proc. Adv. in Neural Inf. Process. Syst.*, Red Hook, NY, USA, 2017, pp. 5998–6008.
- [15] R. E. Bellman, "Dynamic programming treatment of the traveling salesman problem," *J. ACM*, vol. 9, no. 1, pp. 61–63, 1961.

<sup>1</sup>[Online]. Available: <https://github.com/liangxinedu/stepwise>

- [16] Y. Bengio, A. Lodi, and A. Prouvost, "Machine learning for combinatorial optimization: A methodological tour d'hORIZON," *Eur. J. Oper. Res.*, to be published, doi: [10.1016/j.ejor.2020.07.063](https://doi.org/10.1016/j.ejor.2020.07.063).
- [17] H. Dai, B. Dai, and L. Song, "Discriminative embeddings of latent variable models for structured data," in *Int. Conf. Mach. Learn.*, 2016, pp. 2702–2711.
- [18] X. Chen and Y. Tian, "Learning to perform local rewriting for combinatorial optimization," in *Proc. Adv. Neural Inf. Process. Syst.*, 2019, pp. 6281–6292.
- [19] Y. Wu, W. Song, Z. Cao, J. Zhang, and A. Lim, "Learning improvement heuristics for solving routing problems," Dec. 2019, *arXiv:1912.05784*.
- [20] S. Y. Hao Lu and X. Zhang, "A learning-based iterative method for solving vehicle routing problems," in *Proc. 8th Int. Conf. Learn. Representations*, 2020.
- [21] C. K. Joshi, T. Laurent, and X. Bresson, "An efficient graph convolutional network technique for the travelling salesman problem," *arXiv:1906.01227*, 2019.
- [22] D. Selsam *et al.*, "Learning a sat solver from single-bit supervision," in *Proc. Int. Conf. Learn. Representations*, 2018.
- [23] Z. Li, Q. Chen, and V. Koltun, "Combinatorial optimization with graph convolutional networks and guided tree search," in *Proc. Adv. Neural Inf. Process. Syst.*, 2018, pp. 539–548.
- [24] P.-W. Wang, P. L. Donti, B. Wilder, and Z. Kolter, "SATNet: Bridging deep learning and logical reasoning using a differentiable satisfiability solver," in *Proc. Int. Conf. Learn. Representations*, 2019, pp. 6545–6554.
- [25] I. Sutskever, O. Vinyals, and Q. V. Le, "Sequence to sequence learning with neural networks," in *Proc. Adv. Neural Inf. Process. Syst.*, 2014, pp. 3104–3112.
- [26] D. Bahdanau, K. Cho, and Y. Bengio, "Neural machine translation by jointly learning to align and translate," in *Proc. 3rd Int. Conf. Learn. Representations*, San Diego, CA, USA, 2015.
- [27] K. He, X. Zhang, S. Ren, and J. Sun, "Deep residual learning for image recognition," in *Proc. IEEE Conf. Comput. Vis. Pattern Recognit.*, 2016, pp. 770–778.
- [28] S. Ioffe and C. Szegedy, "Batch normalization: Accelerating deep network training by reducing internal covariate shift," in *Proc. Int. Conf. Learn. Representations*, 2015, pp. 448–456.
- [29] O. Vinyals, S. Bengio, and M. Kudlur, "Order matters: Sequence to sequence for sets," in *Proc. 3rd Int. Conf. Learn. Representations*, San Diego, CA, USA, 2015.
- [30] F. Schroff, D. Kalenichenko, and J. Philbin, "FaceNet: A unified embedding for face recognition and clustering," in *Proc. IEEE Conf. Comput. Vis. Pattern Recognit.*, 2015, pp. 815–823.
- [31] D. Applegate, R. Bixby, V. Chvatal, and W. Cook, "Concorde TSP solver," 2006. Online: Available: <http://www.math.uwaterloo.ca/tsp/concorde>
- [32] K. Helsgaun, *An Extension of the Lin–Kernighan–Helsgaun TSP Solver for Constrained Traveling Salesman and Vehicle Routing Problems*. Roskilde: Roskilde University, 2017.
- [33] D. P. Kingma and J. Ba, "Adam: A method for stochastic optimization," in *Proc. 3rd Int. Conf. Learn. Representations*, San Diego, CA, USA, 2014.
- [34] K. Helsgaun, "An effective implementation of the Lin–Kernighan traveling salesman heuristic," *Eur. J. Oper. Res.*, vol. 126, no. 1, pp. 106–130, 2000.
- [35] G. Reinelt, "TSPLIB – A traveling salesman problem library," *ORSA J. Comput.*, vol. 3, no. 4, pp. 376–384, 1991.



**Liang Xin** received the bachelor's degree in civil engineering from Tongji University, Shanghai, China and the master's degree in civil and environmental engineering from Carnegie Mellon University, Pittsburgh, PA, USA. He is currently working toward the Ph.D. degree in computer science at the School of Computer Science and Engineering, Nanyang Technological University, Singapore.

His research interests include deep learning for combinatorial optimization problems.



**Wen Song** received the B.S. degree in automation and the M.S. degree in control science and engineering from Shandong University, China, in 2011 and 2014, respectively, and the Ph.D. degree in computer science from Nanyang Technological University, Singapore, in 2018.

He was a Research Fellow with the Singtel Cognitive and Artificial Intelligence Lab for Enterprises (SCALE@NTU), Singapore. He is currently an Associate Professor with the Institute of Marine Science and Technology, Shandong University, China. His research interests include artificial intelligence, machine learning, planning and scheduling, multiagent systems, and operations research.



**Zhiguang Cao** received the B.Eng. degree in automation from the Guangdong University of Technology, Guangzhou, China, in 2009, the M.Sc. degree in signal processing from Nanyang Technological University, Singapore, in 2012, and the Ph.D. degree in computer science from Interdisciplinary Graduate School, Nanyang Technological University, Singapore, in 2017.

He worked as a Research Fellow with Future Mobility Research Lab, and Energy Research Institute @ NTU (ERI@N), Singapore. He is currently a Research Assistant Professor with the Department of Industrial Systems Engineering and Management, National University of Singapore, Singapore. His research interests include AI and combinatorial optimization problems.



**Jie Zhang** received the Ph.D. degree in computer science from the Cheriton School of Computer Science, University of Waterloo, Canada, in 2009.

He is an Associate Professor with the School of Computer Science and Engineering, Nanyang Technological University, Singapore. During his Ph.D. study, he received the prestigious NSERC Alexander Graham Bell Canada Graduate Scholarship for top Ph.D. students across Canada. His research interests include the design of effective and robust intelligent software agents, through the modeling (trustworthiness, preferences) and simulation of different agents in a wide range of environments, using AI techniques (data mining, machine learning, and probabilistic reasoning) and multiagent technologies.